THE JOURNAL OF BIOLOGICAL CHEMISTRY VOL. 289, NO. 2, pp. 1092–1105, January 10, 2014

Leishmania donovani Prevents Oxidative Burst-mediated Apoptosis of Host Macrophages through Selective Induction of Suppressors of Cytokine Signaling (SOCS) Proteins*[S]

Received for publication, June 24, 2013, and in revised form, October 22, 2013 Published, JBC Papers in Press, November 25, 2013, DOI 10.1074/jbc.M113.496323

Supriya Srivastav[‡], Writoban Basu Ball[‡], Purnima Gupta[§], Jayeeta Giri[§], Anindita Ukil[§], and Pijush K. Das[‡1]

From the [‡]Infectious Diseases and Immunology Division, Council of Scientific and Industrial Research-Indian Institute of Chemical Biology, Kolkata 700032 and the [§]Department of Biochemistry, Calcutta University, Kolkata 700019, India

Background: *Leishmania* inhibits oxidative burst-mediated apoptosis of macrophages during phagocytosis.
Results: *L. donovani* induces (SOCS) 1 and 3, which suppress macrophage apoptosis through thioredoxin-mediated stabilization of protein-tyrosine phosphatases.
Conclusion: *Leishmania* exploits macrophage SOCS proteins for inhibition of apoptosis, thus protecting its niche for survival and replication.
Significance: This study demonstrates a novel anti-apoptotic mediator for parasite infection.

One of the mechanisms for establishment of infection employed by intra-macrophage pathogen-like *Leishmania* is inhibition of oxidative burst-mediated macrophage apoptosis to protect their niche for survival and replication. We tried to elucidate the underlying mechanism for this by using H_2O_2 for induction of apoptosis. *Leishmania donovani*-infected macrophages were much more resistant to H_2O_2-mediated apoptosis compared with control. Although infected cells were capable of comparable reactive oxygen species production, there was less activation of the downstream cascade consisting of caspase-3 and -7 and cleaved poly(ADP)-ribose polymerase. Suppressors of cytokine signaling (SOCS) 1 and 3 proteins and reactive oxygen species scavenging enzyme thioredoxin, known to be involved in stabilization of protein-tyrosine phosphatases, were found to be induced during infection. Induction of SOCS proteins may be mediated by Egr1, and silencing of *Socs1* and *-3* either alone or in combination resulted in reduced thioredoxin levels, enhanced activation of caspases, and increased apoptosis of infected macrophages. The induction of protein-tyrosine phosphatases, thioredoxin, SOCS, and Egr1 in *L. donovani*-infected macrophages was found to be unaffected by H_2O_2 treatment. SOCS knocked down cells also displayed decreased parasite survival thus marking reduction in disease progression. Taken together, these results suggest that *L. donovani* may exploit SOCS for subverting macrophage apoptotic machinery toward establishing its replicative niche inside the host.

Programmed cell death, or apoptosis, is a signal-dependent physiological suicide mechanism that preserves homeostasis by maintaining the delicate balance between cell proliferation and cell death (1). Apart from serving all these diverse spectra of functions, it serves as a defense mechanism against viruses and probably other infectious agents, such as intracellular bacteria and parasites (2). In plants, insects, and mammals, the rapid induction of apoptosis in response to pathogen entry represents an evolutionarily conserved protective response against infections. Conversely, as pathogens are under great selective pressure to defeat the host defense systems, they have evolved a variety of ways to specifically antagonize apoptotic death of the invaded host cell, allowing them more time to replicate (3–5). Moreover, it would be to the advantage of the invading organism to subvert the apoptotic machinery; hence not destroying its niche before egression. Therefore, even though apoptosis, induced in infected cells by cytotoxic immune effector cells, is a critical defense against intracellular pathogens, many viral, bacterial, and protozoan pathogens have developed mechanisms to invade and multiply within host cells without inducing apoptosis (6–10). Various parasites undermine the apoptotic progression that includes *Chlamydia*, *Escherichia coli*, *Mycobacterium tuberculosis*, *Toxoplasma gondii*, *Plasmodium berghei,* and *Leishmania* species (11–17). *Leishmania donovani* was the first parasite reported to enhance host cell viability by inhibiting growth factor deprivation-induced apoptosis. One potential mechanism behind this inhibition has been through the activation of NF-κB and PI3K/Akt pathways (17, 18).

Leishmania species cause a spectrum of diseases ranging from nonlethal cutaneous leishmaniasis (*Leishmania major*) to fatal visceral leishmaniasis (*L. donovani*). The *Leishmania* parasites are internalized by macrophages into phagolysosomes, where they display the remarkable ability to survive and replicate within this hostile environment. However, it is of interest to note that once internalized into macrophages, the parasite has to face severe oxidative stress inside the macrophages due to extensive production of reactive oxygen species (ROS)[2] (19).

* This work was supported by Network Project Grant BSC 0206 and Supra Institutional Project Grant BSC 0114 from the Council of Scientific and Industrial Research and the J. C. Bose Fellowship (Department of Science and Technology), Government of India.
[S] This article contains supplemental Figs. 1–3.
[1] To whom correspondence should be addressed: CSIR-Indian Institute of Chemical Biology, 4 Raja S.C. Mullick Rd., Kolkata 700032, India. Tel.: 91-33-2414-0921; Fax: 91-33-2473-5197; E-mail: pijushdas@iicb.res.in.

[2] The abbreviations used are: ROS, reactive oxygen species; SOCS, suppressors of cytokine signaling; PTP, protein-tyrosine phosphatase; SHP, Src homology; DCFDA, 2′,7′-dichlorofluorescein diacetate; PARP, poly(ADP)-ribose polymerase; Z, benzyloxycarbonyl; fmk, fluoromethyl ketone; pNPP, *p*-nitrophenyl phosphate; *p*NA, *p*-nitroanilide; PI, propidium iodide.

Large quantities of ROS have been implicated as microbicidal agents in pathological situations and ultimately result in apoptosis of the macrophages harboring the pathogen, thereby resulting in parasite clearance (20). Although *Leishmania* promastigotes are susceptible to oxygen intermediates generated *in vitro*, they succeed in establishing infection either by avoiding or resisting the toxic effects of superoxide and other ROS generated during phagocytosis (21, 22). Recent studies have revealed that ROS leads to transient oxidation and inactivation of protein-tyrosine phosphatases (PTPs) that compose a large, structurally diverse family of receptor-like and nontransmembrane enzymes that are specific regulators of signal transduction, which, in conjunction with the protein-tyrosine kinases, exert exquisite control over various biological functions (23, 24). All PTPs contain catalytic cysteine residues on the ROS-sensitive site, and the ROS-mediated oxidation of cysteine residues results in their inactivation. These phenomena are reversible during the redox regulation such that the oxidized PTPs are readily reduced back by thioredoxin and/or glutathione, which act in the ROS scavenging system. In various studies, a role of thioredoxin in cell protection from the ROS-induced apoptosis has been reported in mammalian systems (25, 26). These PTP-stabilizing enzymes such as thioredoxin are reported to act in coordination with members of the suppressors of cytokine signaling (SOCS) family in the inhibition of ROS-mediated apoptotic signaling cascade (27). It has been reported that SOCS suppress cytokine signal transduction by binding to phosphorylated tyrosine residues on cytokine receptor chains, and the physiological importance of SOCS1 and SOCS3 is demonstrated by the lethal phenotypes observed in knock-out mice (28). Silencing of SOCS proteins has been reported to promote apoptosis in various malignancies. Moreover, recent studies have also shown the implication of SOCS-mediated anti-apoptotic signaling in several diseases (29–32). In addition to the modulation of PTPs, the mechanisms of ROS-induced apoptosis involve diverse downstream enzymes, including mitogen-activated protein kinases (MAPKs) and the associated signaling pathways. However, the precise role that different MAPK members play during ROS-induced apoptosis and the mechanistic link between ROS-mediated modulation of PTPs and MAPK activation are not known.

In this study, using hydrogen peroxide as an inducing agent for ROS-mediated apoptosis, we tried to elucidate the mechanism used by the parasite to counteract oxidative burst and the consequent suppression of oxidative burst-mediated host cell apoptosis. Hydrogen peroxide treatment failed to bring about apoptosis of macrophages infected with *L. donovani*. It was observed that although infected cells were capable of ROS production during early hours, there was complete abrogation of the downstream caspase cascade that was found to be mediated by SOCS proteins. Silencing of these proteins resulted in reduced thioredoxin levels and increased apoptosis in infected macrophages through de-activation of PTPs. SOCS knockdown cells also displayed decreased parasite survival, thus marking reduction in disease progression. Taken together, these results suggest that *L. donovani* employs differential induction of host SOCS proteins to subvert macrophage apoptotic machinery triggered by parasite internalization-mediated oxidative burst, thus establishing its replicative niche inside the host.

EXPERIMENTAL PROCEDURES

Cell Culture and Parasites—The pathogenic promastigotes of *L. donovani* strain (MHOM/IN/1983/AG83) were maintained in Medium 199 (Invitrogen) supplemented with 10% fetal calf serum (Invitrogen), 50 units/ml penicillin, and 50 μg/ml streptomycin. The murine macrophage cell line RAW 264.7 was maintained at 37 °C, 5% CO_2 in RPMI 1640 medium (Invitrogen) supplemented with 10% FCS, penicillin (100 units/ml), and streptomycin (100 μg/ml). *In vitro* infection experiments were carried out with the RAW 264.7 cell line using stationary phase promastigotes at a 10:1 parasite/macrophage ratio.

Reagents, Antibodies, and Constructs—All antibodies were from Santa Cruz Biotechnology and Cell Signaling Technology. All other chemicals were from Sigma, unless indicated otherwise.

Apoptosis Detection by Annexin V Staining—RAW 264.7 cells (2×10^6) were infected with *L. donovani* promastigotes for different time periods. One group of infected macrophages for each time point of infection was treated with H_2O_2. After an hour of treatment, the culture media were replaced, and cells were incubated overnight at 37 °C, 5% CO_2. The cells were washed twice with PBS. Apoptosis was then determined using annexin-V-FLUOS staining kit (Roche Applied Science) as per the manufacturer's instructions. Cells were analyzed on FACS Canto II™ cell sorter using 488 nm excitation and 530 nm emissions for FITC and >600 nm for PI fluorescence using FACS Diva software.

Immunoprecipitation and Immunoblotting—Cells were lysed in lysis buffer (Cell Signaling Technology), and the protein concentrations in the cleared supernatants were estimated using a protein assay (Bio-Rad). Immunoprecipitation was performed as described previously (33). Briefly, pre-cleared cell lysates (500 μg) were incubated overnight with specific primary antibody at 4 °C. For co-immunoprecipitation studies, pull-down with unrelated antibodies served as control. 25 μl of protein A/G plus agarose beads (Santa Cruz Biotechnology) were added to the mixture and incubated for 4 h at 4 °C. Immune complexes were collected and washed three times with ice-cold lysis buffer and once with lysis buffer without Triton X-100. The immunoprecipitated samples and cell lysates were resolved by 10% SDS-PAGE and then transferred to nitrocellulose membrane (Millipore). 30 μg of protein from the whole cell lysate of each sample were loaded as input. The membranes were blocked with 5% BSA in wash buffer (TBS, 0.1% Tween 20) for 1 h at room temperature and probed with primary antibody overnight at dilution recommended by the suppliers. Membranes were washed three times with wash buffer and then incubated with alkaline phosphatase-conjugated secondary antibody and detected by hydrolysis of 5 bromo-4-chloro-3′-indolylphosphate chromogenic substrate according to the manufacturer's instructions.

Estimation of ROS Production—Intracellular ROS generation was measured using the oxidant sensitive green fluorescent dye 2′,7′-dihydrodichlorofluorescein diacetate

(H_2DCFDA) (Molecular Probes). Measurement of fluorescence in cells was made by counting at least 10,000 events/test using a FACScalibur flow cytometer (BD Biosciences), with a fluorescein isothiocyanate filter, and the cells were gated out based on their fluorescent property. Samples were examined by FACScalibur, and the results were analyzed using CellQuest software (BD Biosciences).

Phosphatase Assay—Macrophages were lysed in PTP lysis buffer (50 mM Hepes, pH 7.4, containing 0.5% Triton X-100, 10% glycerol, 1 mM benzamidine, 10 μg/ml aprotinin, 10 μg/ml leupeptin, and 2 μg/ml pepstatin A) and kept on ice for 45 min. Lysates were cleared by centrifugation, and protein content was determined by protein assay (Bio-Rad). 10 μg of protein extract were incubated in phosphatase reaction buffer (50 mM Hepes, pH 7.5, 0.1% 2-mercaptoethanol, 10 mM pNPP) for 30 min. Absorbance was read at 405 nm. In a separate set of experiments, PTP activity was further determined by the capacity of protein lysates to dephosphorylate a monophosphorylated phosphotyrosine peptide substrate (TRDIpYETDYYRK) for 10 min at 37 °C. Free inorganic phosphate was detected with malachite green (Sigma), and absorbance was taken at 620 nm. To evaluate specific activities of SHP-1, PTP1B, SHP-2, and CD45, the proteins were immunoprecipitated using respective antibodies, and specific PTP activity was then evaluated by pNPP hydrolysis as described above. Nonspecific hydrolysis of pNPP by lysates was assessed in nonimmune IgG immunoprecipitates and subtracted from the values obtained for enzyme immunoprecipitates.

Real Time PCR—Total RNA from RAW 264.7 cells was isolated using the RNeasy mini kit (Qiagen) according to the manufacturer's instructions. 1 μg of DNA was used as template for cDNA synthesis using the SuperScript first strand synthesis system for the RT-PCR kit (Invitrogen). Quantitative real time PCRs (ABI 7500 Fast Real Time PCR system, Applied Biosystems) were performed using TaqMan Fast Universal PCR master mix (Applied Biosystems). TaqMan probes for *Socs1, Socs2, Socs3*, and CIS were purchased from Applied Biosystems. The ABI 7500 Fast Sequence detector was programmed with the following PCR amplification conditions: 40 cycles of 95 °C for 15 s and 60 °C for 1 min. β-Actin was chosen as an internal control for variability in amplification because of differences in initial mRNA concentrations. Relative quantitation was performed using the comparative $\Delta\Delta C_t$ method, and data were normalized to β-actin mRNA levels and expressed as a fold change compared with uninfected controls.

siRNA Transfection—RAW 264.7 cells (2×10^6) were transfected with 1 μg of either Egr1 or SHP1 or PTP1B or thioredoxin or SOCS1 and/or SOCS3 siRNA according to the manufacturer's instructions (Santa Cruz Biotechnology). Scrambled siRNA was used as control. Following silencing, cells were infected with *L. donovani* promastigotes as described earlier.

Caspase-3 Activity Assay—Cells were washed twice with ice-cold PBS, resuspended in 50 μl of ice-cold lysis buffer (1 mM DL-dithiothreitol, 0.03% Nonidet P-40 (v/v), in 50 mM Tris, pH 7.5), kept on ice for 30 min, and finally centrifuged at 14,000 × *g* for 15 min at 4 °C. 10 μg of total protein was incubated with the caspase-3 substrate (Ac-DEVD-*p*NA) for 1 h at 37 °C. The absorption was measured by spectrometry at 405 nm.

Electrophoretic Mobility Shift Assays (EMSA)—10 μg of nuclear extracts from control as well as treated cells were preincubated with 1 μg of poly(dI-dC) in a binding buffer (25 mM Hepes, pH 7.9, 0.5 mM EDTA, 0.5 mM DTT, 1% Nonidet P-40, 5% glycerol, and 50 mM NaCl) for 10 min at room temperature. 0.5 ng of [α-^{32}P]dCTP-labeled Egr1 oligonucleotide probe was then added to the reaction mixture followed by incubation for 30 min. Oligonucleotide probe with a mutated Egr1-binding site (Santa Cruz Biotechnology) was used for competition experiments. The DNA-protein complex was then electrophoresed on 6% nondenaturing polyacrylamide gels in 0.5× TBE buffer (50 mM Tris, 50 mM borate, and 1 mM EDTA) and analyzed by autoradiography.

Fluorescence Microscopy—Macrophages (5×10^5) were plated onto 18-mm^2 coverslips kept in 30-mm Petri plates and cultured overnight. The cells were then infected with *L. donovani* promastigotes, washed twice in PBS, and fixed with methanol for 15 min at room temperature. The cells were then permeabilized with 0.1% Triton X-100 and incubated with Egr1 antibody for 1 h at 4 °C. After washing, coverslips were incubated with Texas Red-conjugated secondary antibody (1 h, 4 °C). The cells were then stained with 4′,6-diamidino-2-phenylindole (DAPI, 1 μg/ml) in PBS plus 10 μg/ml RNase A to label the nucleus, mounted on slides, and visualized under Olympus BX61 microscope at a magnification of 1000, and the images thus captured were processed using ImagePro Plus (Media Cybernetics).

Chromatin Immunoprecipitation (ChIP) Assay—Cells were cross-linked with 1% formaldehyde and harvested into lysis buffer (1% SDS, 10 mM EDTA, 50 mM Tris-HCl, pH 8.0, and 1× protease inhibitor mixture) and sonicated, followed by immunoprecipitating with rabbit anti-Egr1 antibody. Immunoprecipitation with a normal rabbit IgG served as a negative control. Immunoprecipitated cell lysates were incubated with protein A/G plus agarose, washed, and then heated at 65 °C for 1.5 h to reverse the cross-linking. DNA fragments were purified, and PCR amplification was performed using 5 μl of DNA (recovered from ChIP) with 35 cycles of denaturation at 95 °C (30 s), annealing at 60 °C (50 s), and extension at 72 °C (50 s) with a final extension at 72 °C for 10 min, and amplified PCR products were analyzed by electrophoresis on a 1.5% agarose gel. The following primer pairs were used to amplify putative Egr1-binding sites in the *Socs1* and *Socs3* promoter regions, respectively. SOCS1 sense 5′-CGGGGCCTCAGTTTCTCC-3′ and antisense 5′-ATCAGGCTCTTAAACCAGGCA-3′, and SOCS3 sense 5′-TGAATAAGGAGCCCCACAAC-3′ and antisense 5′-TACCTAGTCCCGAAGCGAAAT-3′.

Densitometric Analysis—Densitometric analyses for all experiments were carried out using QUANTITY ONE software (Bio-Rad). Band intensities were quantitated densitometrically, and the values were normalized to endogenous control and expressed in arbitrary units. The ratios of optical density of particular bands/endogenous control are indicated as bar graphs adjacent to figures.

Statistical Analysis—Data shown are representative of at least three independent experiments unless otherwise stated as *n* values given in the legend. Macrophage cultures were set in triplicate, and the results are expressed as the mean ± S.D.

Student's *t* test was employed to assess the statistical significance of differences among a pair of data sets with a *p* value of <0.05 considered to be significant.

RESULTS

L. donovani Inhibits H_2O_2-induced Apoptosis of Host Macrophages during Phagocytosis—Internalization of a pathogen into macrophages generally causes a huge oxidative burst that results in apoptosis of host cells toward clearance of pathogen burden (20). To determine whether the intra-macrophage parasite *L. donovani* can evade this strategy of host defense, thus protecting its niche for survival and replication, we measured the ROS production in macrophages infected with *L. donovani* during early hours of infection. To this end, RAW 264.7 cells were infected with *L. donovani* promastigotes for the indicated time periods, washed with PBS, and incubated for 30 min with the green fluorescent dye H_2DCFDA, and fluorescence levels of 50,000 cells were counted. A gate was established that delineated approximately the upper 5% of fluorescent cells. *L. donovani* infection was found to cause 68.8 ± 8.4, 71.6 ± 5.8, 61.6 ± 7.4, and 40.2 ± 3.2% ROS production in RAW 264.7 macrophages at 5, 10, 15, and 30 min post-infection, respectively (Fig. 1*A*). To determine whether this initial oxidative outburst could lead to macrophage apoptosis, cells were infected with *L. donovani* for the indicated time points, washed to remove un-internalized parasites, and incubated overnight at 37 °C, and the percentage of apoptotic cells was measured by annexin V-PI flow cytometric analysis. Host cell apoptosis in infected macrophages was found to be considerably higher at 5 min of infection (55.4 ± 7.8% annexin V-positive cells, $p < 0.0001$), which was significantly reduced during later time points (38.8 ± 5.9%, $p < 0.0001$, and 6.9 ± 0.8%, $p < 0.0002$, at 10 and 15 min, respectively) (Fig. 1*B*). To determine whether this amount of ROS produced during early hours of *L. donovani* infection was capable of causing macrophage apoptosis, cells were administered with the indicated concentrations of H_2O_2 to mimic the initial oxidative burst condition in the case of *L. donovani* during 5–30 min of infection. Interestingly, 62.1 ± 8.1% of ROS produced by 200 μM H_2O_2 (Fig. 1*C*), which was very close to that produced by *L. donovani* at 15 min post-infection (61.6%), could cause a significant induction in apoptotic macrophage populations (68.9 ± 5.2% annexin V-positive cells, $p < 0.0001$) (Fig. 1*D*) as compared with 6.9% in case of *L. donovani* infection. Because *L. donovani* could inhibit host cell apoptosis despite significant ROS production during phagocytosis, we administered H_2O_2 (400 μM for 1 h) and compared the induction of apoptosis in normal and *L. donovani*-infected macrophages at various time points of infection. H_2O_2 exposure resulted in 79.6 ± 9.7 annexin V-positive cells in the case of normal macrophages ($p < 0.0002$) (Fig. 1*E*). In contrast, *L. donovani*-infected cells showed a much lower extent of apoptosis on exposure to H_2O_2 (11.6 ± 0.8, 8.2 ± 1.3, 7.7 ± 0.4, 8.8 ± 1.3, and 7.7 ± 0.9% annexin V-positive cells at 2, 4, 6, 12 and 24 h after infection) (Fig. 1*E*). To investigate whether the inhibition in host cell apoptosis was dependent upon pathogen internalization, cells were administered with cytochalasin D (which prevents the uptake but not the attachment of the parasite) prior to infection. Cytochalasin D treatment (2 μM) caused 54.7 ± 7.7, 70.7 ± 4.9, and 82.3 ± 5.8% reduction in internalized parasites as compared with untreated infected cells at 2, 4, and 6 h post-infection, respectively ($p < 0.01$) (Fig. 1*F*). Parasite-mediated suppression of apoptosis was reversed on treating the cells with cytochalasin D. Cytochalasin D treatment in macrophages showed a much higher extent of apoptosis than infected macrophages (33.1 ± 6.2, 35.1 ± 5.1, and 50.7 ± 5.9% more apoptotic cells as compared with *L. donovani*-infected macrophages at 2, 4, and 6 h post-infection, $p < 0.01$) (Fig. 1*G*). This suggests that internalization of the parasite is a necessary prerequisite for suppression of host cell apoptosis. To determine whether this inhibition of apoptosis was mediated through the inhibition of ROS production by the parasite, we measured ROS levels at similar time points in H_2O_2-administered infected cells. *L. donovani*-infected cells were found to produce significant levels of ROS up to 6 h, with a maximum of 55.0 ± 3.7% at 2 h post-infection (Fig. 1*H*). ROS production by macrophages incubated for various time periods (2–24 h) was found to be comparable with that in control cells (0 h of incubation) after treatment with H_2O_2 for 1 h (supplemental Fig. 1) thereby suggesting that merely incubating cells before H_2O_2 treatment does not make them refractory to ROS production. Inhibition of ROS generation may therefore be attributed to parasite infection. Taken together, these results suggest that *L. donovani* can successfully counteract oxidative burst-mediated apoptosis in macrophages, which is not mediated by inhibition of ROS production.

L. donovani Infection Inhibits the Caspase Cascade through De-phosphorylation of MAPKs—To ascertain whether H_2O_2-induced apoptotic response was mediated by MAPKs, we sought to determine the phosphorylation-mediated activation of MAPKs in H_2O_2-treated infected cells. There was significant decrease in phosphorylated forms of p38 (41.4, 84.1, and 73.4% reduction at 2, 4, and 6 h post-infection, respectively, as compared with H_2O_2-administered control macrophages, $p < 0.05$) (Fig. 2*A*, *left panel*). The levels of phospho-ERK1/2 in *L. donovani*-infected cells were found to be reduced significantly after 4 h and continued to decrease until 24 h (68.7 and 73.7% reduction in p-ERK1 and p-ERK2 at 6 h post-infection, $p < 0.001$) upon H_2O_2 treatment as compared with H_2O_2-treated uninfected cells (Fig. 2*A*, *left panel*). However, reduction in p-JNK was observed only at 2 h post-infection (54.6% reduction, $p < 0.001$) (Fig. 2*A*, *left panel*). High basal levels of p-p38, p-ERK, and p-JNK obtained in H_2O_2-treated normal macrophages (Fig. 2*A*, *left panel*) may be attributed to peroxide treatment as H_2O_2-untreated normal macrophages did not show any phosphorylation of p38, ERK, and JNK (supplemental Fig. 2). The phosphorylation of all three MAPKs was markedly abrogated in *L. donovani*-infected cells in the absence of H_2O_2 treatment (Fig. 2*A*, *right panel*), suggesting that *Leishmania* strongly inhibits MAPK activation. We further checked the activation of caspases following *L. donovani* infection and found that whereas control macrophages following H_2O_2 treatment showed high levels of active initiator caspase-9 and -7, there was a marked reduction (56.4 and 31.1% reduction, $p < 0.05$) of these caspases at 6 h post-infection with a gradual increase in the level of pro-caspases (Fig. 2*B*, *left panel*). However, *L. donovani* infection in the absence of H_2O_2 treatment depicted no

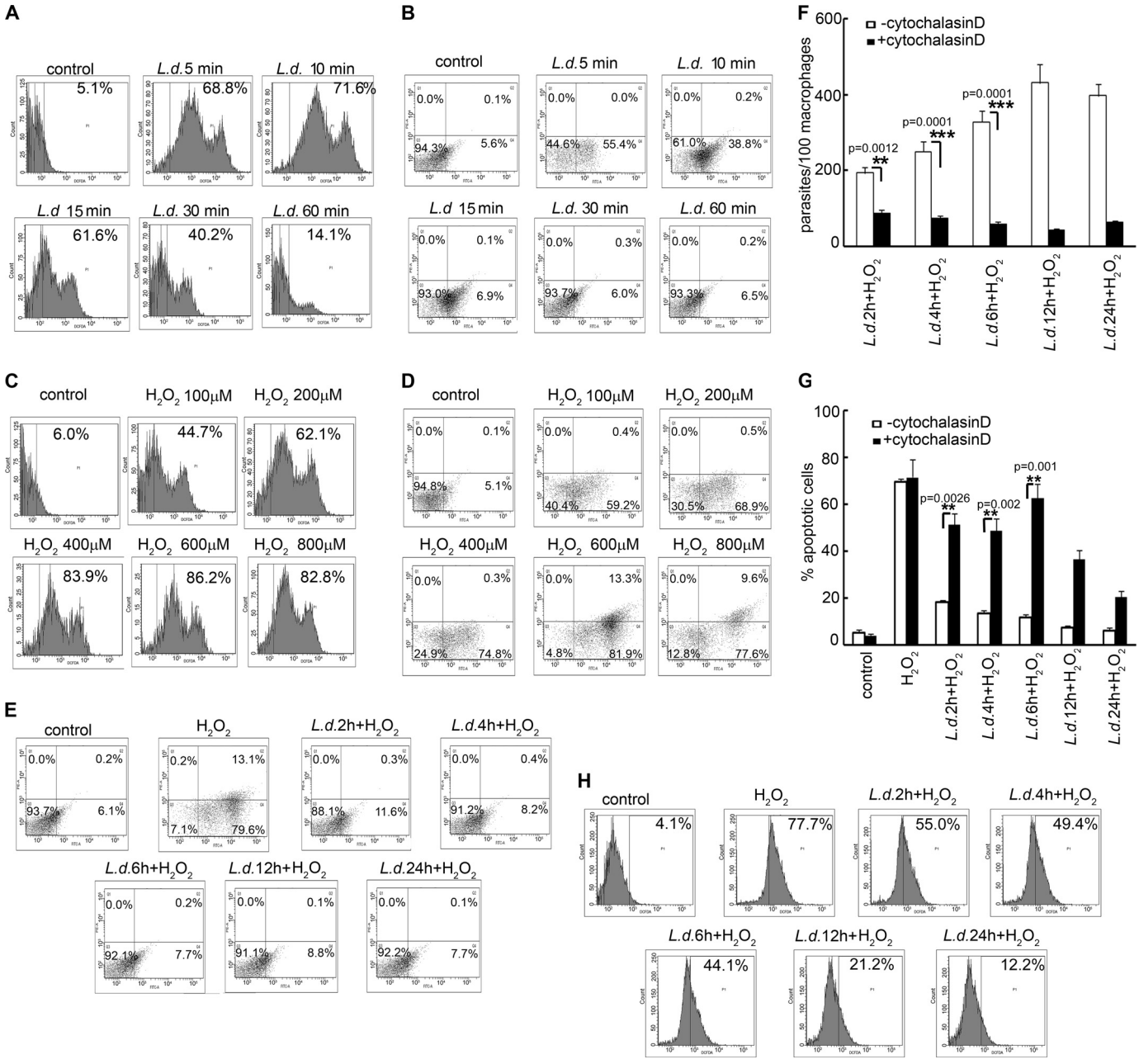

FIGURE 1. **Effect of *L. donovani* infection on macrophage ROS generation and apoptosis.** *A, C,* and *H,* macrophages were either infected with *L. donovani* (*L.d.*) promastigotes with a parasite/macrophage ratio of 10:1 for the indicated time periods (*A*) or treated with various concentrations of H_2O_2 for 1 h (*C*) or infected with promastigotes followed by treatment with H_2O_2 (400 μM) for 1 h (*H*). Cells were washed, and ROS generation was measured by H_2DCFDA staining followed by flow cytometric analysis. The H_2DCFDA-positive cells are indicated as the percentage of gated cells. *B, D,* and *E,* macrophages were either infected with *L. donovani* promastigotes (*B*) or treated with various concentrations of H_2O_2 for 1 h (*D*) or infected with promastigotes followed by treatment with H_2O_2 (400 μM) for 1 h (*E*). Cells were washed and incubated overnight at 37 °C, and the extent of apoptosis was analyzed by annexin V-tagged FITC-PI flow cytometry. Dual parameter dot plot of FITC fluorescence (*x* axis) *versus* PI fluorescence (*y* axis) is represented as logarithmic fluorescence intensity. Quadrants are as follows: *upper left,* necrotic cells; *lower left,* live cells; *lower right,* apoptotic cells; *upper right,* necrotic or late phase of apoptotic cells. *F* and *G,* control or cytochalasin D (2 μM)-pretreated RAW 264.7 cells were infected with *L. donovani* promastigotes for different time periods as indicated. The number of parasites per 100 macrophages was evaluated by Giemsa staining (*F*), and apoptosis was quantified by flow cytometry (*G*). Results are representative of three individual experiments, and the *error bars* represent mean ± S.D. ($n = 3$). **, $p < 0.01$; ***, $p < 0.001$ by Student's *t* test.

cleavage of pro-caspase-9 and -7 (Fig. 2*B*, *right panel*). We further checked the expression and activity of caspase-3, which is the main effector caspase involved in the apoptotic signaling cascade. There was a significant reduction in cleaved caspase-3 expression (21.7, 59.8, and 80.4% reduction at 2, 4, and 6 h post-infection, respectively) (Fig. 2*C*, *left panel*) with a concomitant decrease in its activity (44.6, 52.1, and 68.3% reduction at 2, 4, and 6 h post-infection, respectively, $p < 0.01$) (Fig. 2*D*) as compared with control cells after H_2O_2 treatment, further confirming the inhibition of ROS-mediated apoptosis by *Leishmania*. Administration of caspase-9 inhibitor Z-LEHD-fmk to infected macrophages before H_2O_2 treatment did not result in further increases in the levels of downstream pro-caspase-7 and -3 (Fig. 2*E*), thereby suggesting that the gradual increase in the

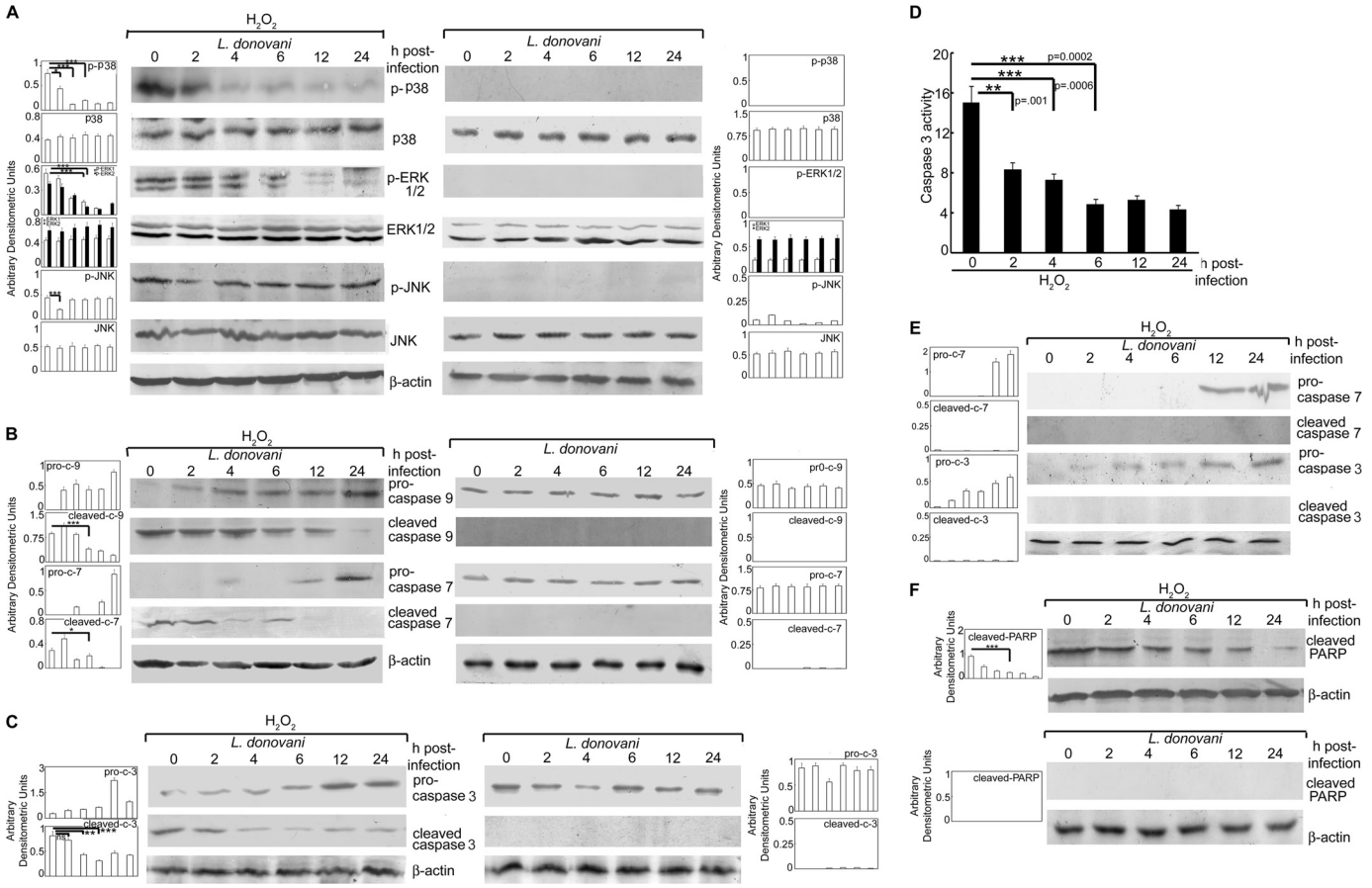

FIGURE 2. **Effect of *L. donovani* infection on MAPK activity and caspase cascade.** *A–C* and *F,* macrophages were infected with *L. donovani* for the indicated time periods followed by either H_2O_2 treatment for 1 h or not. Cells were washed and expression of various MAPKs (*A*), pro- and cleaved forms of caspase-9 and -7 (*B*), pro- and cleaved forms of caspase-3 (*C*), and cleaved PARP (*F*) were evaluated by immunoblotting with respective antibodies. *D,* infected cells were treated with H_2O_2 for 1 h and total cellular extracts (10 μg of protein per sample) were used to determine caspase-3 activity using Ac-DEVD-*p*NA as substrate. *E,* infected cells were treated with Z-LEHD-fmk (50 μM) for 1 h followed by H_2O_2 treatment for 1 h. Expression of pro- and cleaved forms of caspases-3 and -7 were determined by Western blotting. Results are representative of three individual experiments, and the *error bars* represent mean ± S.D. ($n = 3$). *ns,* not significant. *, $p < 0.05$; **, $p < 0.01$; ***, $p < 0.001$ by Student's *t* test.

level of pro-caspases observed post-infection (Fig. 2, *B* and *C*) was not due to new synthesis. However, the cleavage of these two caspases was markedly abrogated in the presence of Z-LEHD-fmk suggesting that the stabilization of pro-caspases during *L. donovani* infection may be due to the blockage of their proteolytic cleavage. This was also supported by the fact that an increase in the level of pro-caspases coincided with the gradual decrease in active forms of respective caspases (Fig. 2, *B* and *C*). Moreover, *L. donovani* infection also led to reduction in cleaved PARP levels (73.3% reduction at 6 h post-infection, $p < 0.0001$) (Fig. 2*F*) as compared with control cells after H_2O_2 treatment. *Leishmania* infection at similar time points, in the absence of peroxide, resulted in almost complete inhibition of the cleavage of both caspase-3 and PARP (Fig. 2, *C, right panel,* and *F, lower panel*) further suggesting that *L. donovani* suppresses the MAPK-mediated apoptotic signaling cascade independent of H_2O_2 administration. These results suggested that *L. donovani* infection could modulate ROS-dependent caspase cascade thus protecting host cells from oxidative burst-mediated apoptosis.

L. donovani Induces Macrophage PTP Activity through SOCS-mediated Induction of Thioredoxin—Considering the kinase-phosphatase balance involved in maintaining cellular homeostasis and decreased phosphorylation of ERK and p38 in *L. donovani*-infected cells after H_2O_2 treatment, we sought to determine the total PTP activity in macrophages following infection. Macrophages were analyzed for PTP activity by the capacity of total cell lysates to dephosphorylate pNPP as well as a synthetic tyrosine monophosphorylated peptide substrate. There was significant increase in PTP activity (4.8-, 6.4-, and 5.9-fold at 2, 4, and 6 h post-infection, $p < 0.001$) upon H_2O_2 treatment as compared with H_2O_2-treated uninfected cells (Fig. 3*A*). Infection of macrophages in the absence of H_2O_2 also showed induction in PTP activity (5.2-, 6.7-, and 6.1-fold at 2, 4, and 6 h post-infection, $p < 0.001$), which was comparable with that obtained after H_2O_2 treatment (Fig. 3*A*). Similar trends were noted in case of specific PTP activity as observed by the dephosphorylation of synthetic tyrosine monophosphorylated peptide (Fig. 3*B*). We then checked the individual activity and protein level expression of PTPs known to be involved in the ROS-mediated signaling cascade like SHP-1, SHP-2, CD45, and PTP1B (Fig. 3*C*). Of all the PTPs tested, the activities of SHP-1 and PTP1B were found to be significantly elevated reaching a maximum of 5.6-fold at 6 h post-infection for SHP-1 and 6.3-fold at 4 h post-infection for PTP-1B ($p < 0.001$) (Fig. 3*C*). Protein expression levels of these two proteins were also increased in H_2O_2-treated infected cells (Fig. 3*D*, *left panel*). *L.*

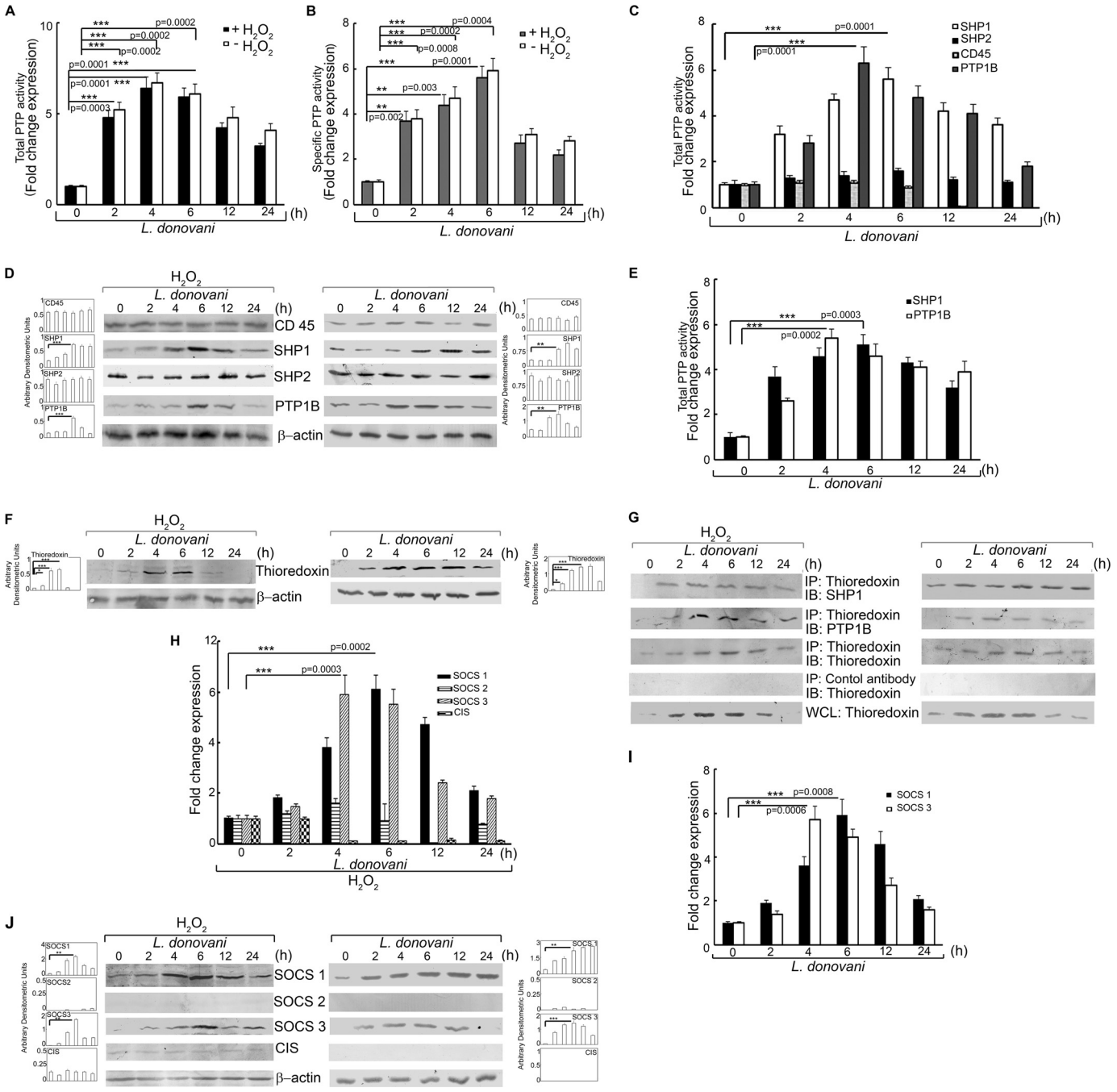

FIGURE 3. **Effect of *L. donovani* infection on PTP activity, thioredoxin, and SOCS expression.** Macrophages were infected with *L. donovani* for the indicated time periods. One group of infected macrophages from each time point was subjected to H_2O_2 treatment for 1 h. *A* and *B,* total and specific PTP activities were evaluated by the capacity of cell lysates to hydrolyze pNPP (*A*) or a synthetic tyrosine phosphopeptide (*B*). Absorbance values were taken at 405 and 620 nm, respectively. *C* and *E,* activity of the indicated PTPs were determined by the capacity of immunoprecipitated samples to hydrolyze pNPP in the presence (*C*) and absence (*E*) of H_2O_2. Results are expressed as the relative increase (*n*-fold) over PTP activity in control cells. *D* and *F,* cells were processed as above and then subjected to Western blotting with respective antibodies for various PTPs (*D*) and thioredoxin (*F*). *G,* cells processed as above were immunoprecipitated with anti-thioredoxin antibody followed by immunoblotting with the indicated antibodies. 30 μg of each sample was loaded as a whole cell lysate input control. *H–J,* expression of various SOCS proteins was determined at mRNA levels in the presence (*H*) and absence (*I*) of H_2O_2 and protein level in the presence (*J, left panel*) and absence (*J, right panel*) of H_2O_2. *IP*, immunoprecipitation using the indicated antibody; *IB,* immunoblot analysis using the indicated antibody; *WCL,* whole cell lysate. Results are representative of three individual experiments, and the *error bars* represent mean ± S.D. ($n = 3$). *, $p < 0.05$; **, $p < 0.01$; ***, $p < 0.001$ by Student's *t* test.

donovani infection in the absence of H_2O_2 also depicted a similar pattern of induction for SHP1 and PTP1B, with a maxima of 5.1-fold at 6 h post-infection for SHP1 and 5.4-fold at 4 h post-infection for PTP1B (Fig. 3*E*). The protein level expressions of both SHP1 and PTP1B were also elevated during infection in the absence of peroxide treatment, thereby suggesting that PTP induction by *Leishmania* might be independent of H_2O_2 treatment (Fig. 3*D*, *right panel*). Because thioredoxin is known to have a role in stabilizing the PTPs, we sought to determine whether *L. donovani* infection had any effect on macrophage

thioredoxin levels. Following H_2O_2 treatment, *L. donovani*-infected macrophages showed significantly enhanced expression of thioredoxin (2.1-, 8.6-, and 9.1-fold as compared with control macrophages at 2, 4, and 6 h post-infection, $p < 0.05$) (Fig. 3*F*, *left panel*). Although infected macrophages (without H_2O_2 treatment) demonstrated similar thioredoxin levels at 2, 4, and 6 h post-infection (Fig. 3*F*, *right panel*), thioredoxin induction was found to persist up to 24 h in the absence of peroxide as compared with infected H_2O_2-treated cells where this was considerably reduced after 6 h of infection. We then checked for the role of thioredoxin in the regulation of PTP activity by studying the molecular interaction between them. Co-immunoprecipitation studies revealed strong association of thioredoxin with both SHP-1 and PTP1B at 4 and 6 h post-infection as compared with control cells both in the presence and absence of H_2O_2 (Fig. 3*G*, *left* and *right panel*). Because thioredoxin is known to be regulated by members of SOCS family of proteins, which play a substantial role in the regulation of ROS-mediated apoptotic signaling cascade, we studied whether *Leishmania* could modulate the expression levels of SOCS proteins under H_2O_2 treatment. Real time PCR analysis of various members of the SOCS family proteins revealed marked elevation in mRNA levels of *Socs1* and *Socs3* with maximum levels (6.1-fold at 6 h for *Socs1* and 5.9-fold at 4 h for *Socs3*, respectively, $p < 0.001$) (Fig. 3*H*) without any apparent alteration in the expression levels of *Socs2* and CIS. Similar induction of SOCS1 and SOCS3 expression was also observed at protein levels (Fig. 3*J*, *left panel*) as studied by immunoblot analysis with maximum expression at 6 h post-infection ($p < 0.01$). However, although the induction of SOCS1 was found to be stable up to 12 h, SOCS3 expression was short lived as seen by the sharp reduction in the level of this protein after 6 h of infection. Moreover, both *Socs1* and *Socs3* were induced in *L. donovani*-infected macrophages even in the absence of peroxide treatment with a maxima of 5.9- and 5.7-fold at mRNA levels at 6 and 4 h post-infection, respectively (Fig. 3*I*). Similar induction was revealed at protein levels (Fig. 3*J*, *right panel*), thereby suggesting that H_2O_2 treatment may not be required for the induction of SOCS proteins by *Leishmania*. These results suggest that *L. donovani* may exploit host SOCS1 and SOCS3 to induce thioredoxin thereby enhancing the activity of PTP.

Transcriptional Regulation of SOCS Proteins by L. donovani—The Egr group of transcription factors is known to regulate the transcription of SOCS family members, and therefore we checked for the expression of Egr1 at both protein and mRNA levels. It was interesting to note that Egr1 mRNA expression was induced in infected macrophages (1.7-, 3.9-, and 5.7-fold over control at 2, 4, and 6 h post-infection, $p < 0.05$), which coincided with SOCS induction (Fig. 4*A*). A similar trend was observed for infected cells in the absence of H_2O_2 (Fig. 4*A*). Induction of Egr1 protein expression was found to be comparable in *L. donovani*-infected macrophages in the presence and absence of H_2O_2 (Fig. 4*B*, *left* and *right panels*). This activation was further ascertained by the nuclear translocation of Egr1 as observed by fluorescence microscopy using anti-Egr1 antibody. In control macrophages, with or without H_2O_2 treatment, the signal for Egr1 was distributed throughout the cell but did not co-localize with DAPI-stained nuclei indicating its cytosolic localization (Fig. 4*C*). On the contrary, *L. donovani* infection for 6 h resulted in an increase in the nuclear localization of Egr1 (irrespective of H_2O_2 treatment) as evident by markedly enhanced co-localization of Egr1 signal (red) with DAPI-stained nuclei (*blue*) (Fig. 4*C*). Because the binding of a transcription factor to DNA is necessary for regulating the transcription of a gene, we checked for the Egr1-DNA binding. Analysis of DNA-protein interaction through EMSA depicted strong Egr1-DNA binding (Fig. 4*D*) at 6 h post-infection, indicating that Egr1 may have a role in elevated expression of SOCS proteins following *Leishmania* infection. To further ascertain the nuclear translocation of Egr1, we analyzed the expression of Egr1 at a protein level in both nuclear and cytosolic fractions. The results showed 3.8- and 3.7-fold more protein expression in nuclear fractions at 6 h post-infection in the case of *L. donovani* infection and *L. donovani* + H_2O_2 treatment, respectively, as compared with control (Fig. 4*F*, *right* and *left panels*). However, although Egr1 levels persisted in the nuclear fraction of *L. donovani*-infected macrophages until 24 h post-infection (Fig. 4*F*, *right panel*), the level decreased considerably after 6 h of infection in the case of H_2O_2 treatment (Fig. 4*F*, *left panel*). This might be the reason why DNA-protein binding was not observed at 12 and 24 h post-infection in Fig. 4*D*. However, we obtained DNA-protein binding up to 24 h post-infection in absence of H_2O_2 (Fig. 4*G*), thereby suggesting that H_2O_2 may exercise a feedback control over Egr1-DNA binding during *L. donovani* infection. Competition experiments using the Egr1 probe with a mutated binding site resulted in complete abrogation of DNA-protein interaction demonstrating the specificity of Egr1-DNA binding (Fig. 4, *E* and *H*). Next, we examined the effect of *L. donovani* infection on the binding of Egr1 to *Socs1* and *Socs3* promoter regions through ChIP. We found a detectable increase in Egr1 binding to the *Socs1* promoter (Fig. 4*I*). Egr1 binding was increased in a time-dependent manner upon *L. donovani* infection. However, the binding of Egr1 to *Socs3* promoter was much less as compared with *Socs1* (Fig. 4*J*). Replacement of Egr1 antibody with control IgG in the ChIP assay failed to yield any amplicon suggesting the specificity of the experiment (Fig. 4, *I* and *J*, *lower panels*). To validate the role of Egr1 in the induction of SOCS in infected macrophages, we used an *in vitro* siRNA knockdown system for Egr1. As seen in Fig. 4*K*, Egr1 was effectively down-regulated by siRNA (88.1% reduction in expression as compared with control siRNA-treated cells, $p < 0.001$). Egr1 knockdown cells showed markedly decreased expression of SOCS1 (66.7% reduction as compared with control siRNA-treated cells, $p < 0.01$) (Fig. 4*L*). However, inhibition of Egr1 resulted in merely 30.4% reduction ($p < 0.05$) in SOCS3 expression (Fig. 4*L*). These results suggest that induction of SOCS1 and SOCS3 may be mediated by Egr1.

Effect of SOCS Inhibition on Thioredoxin-mediated Apoptotic Signaling during L. donovani Infection—To investigate whether induction of SOCS1 and SOCS3 was associated with an increase in thioredoxin-mediated PTP activity, an siRNA-mediated knockdown system was used. Macrophages were administered with either SOCS1 or SOCS3 siRNA alone or in combination, and the efficacy of siRNA treatment was determined by assessment of protein expressions by Western blotting. As seen in Fig. 5, *A* and *B*, expressions of both SOCS1 and SOCS3 were consider-

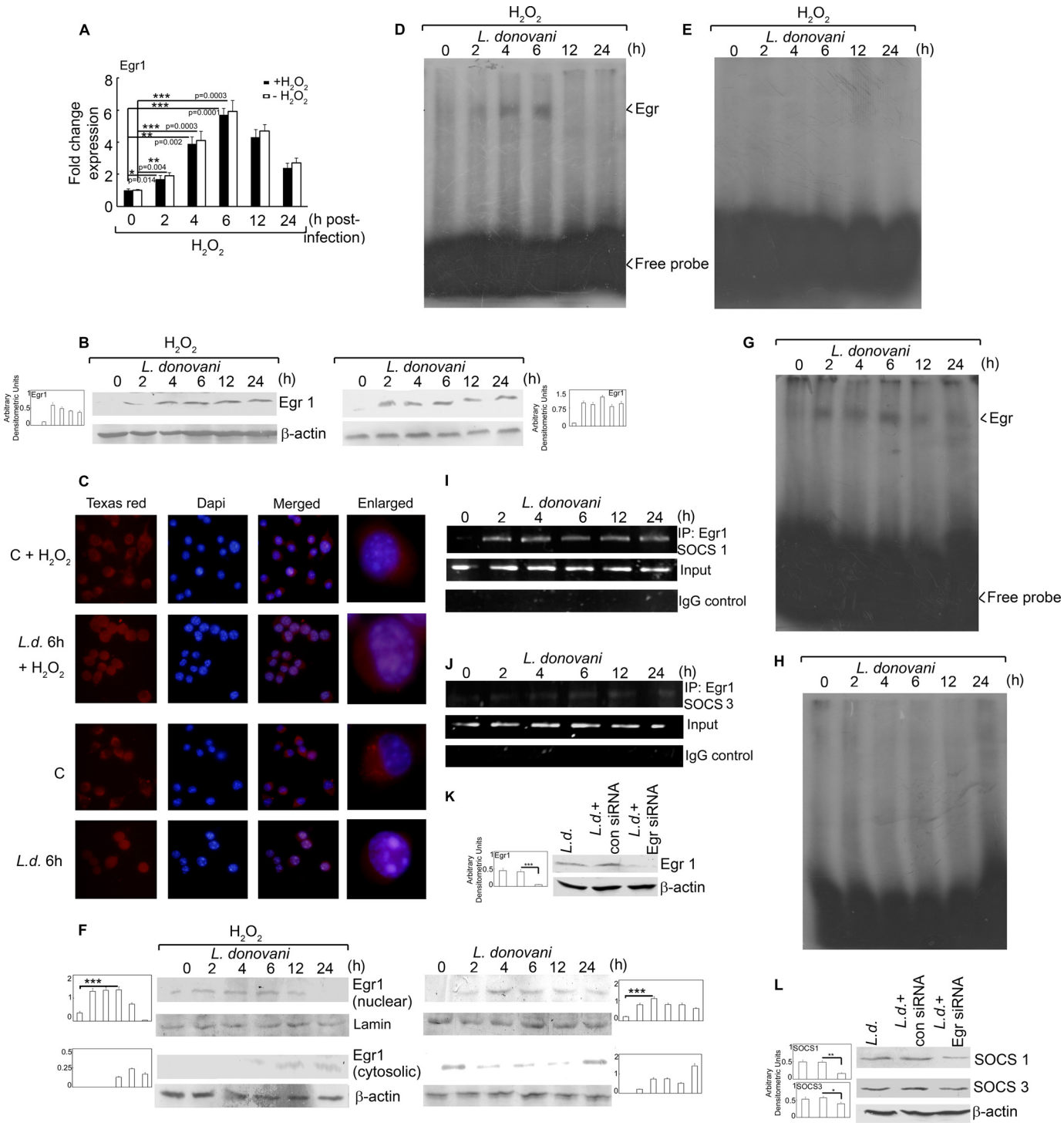

FIGURE 4. **Transcriptional regulation of SOCS proteins.** Macrophages were infected with *L. donovani* for the indicated time periods. One group of infected macrophages from each time point was subjected to H_2O_2 treatment for 1 h. *A* and *B,* Egr1 expression was determined at the mRNA level (*A*) and protein level (*B*) by real time PCR and Western blotting respectively. *C,* cells were stained with anti-Egr1 monoclonal antibody followed by secondary Texas Red-conjugated antibody. Nuclei were stained with DAPI, and cells were analyzed under fluorescence microscope. *D, E, G,* and *H,* labeled Egr1 probe (*D* and *G*) or Egr1 probe with a mutated binding site (*E* and *H*) was incubated with nuclear extracts prepared from cells treated as above. DNA binding was analyzed by EMSA. *F,* cells were treated as above; nuclear and cytosolic extracts were prepared, and expression of Egr1 was analyzed by immunoblotting. *I* and *J,* cells were infected with *L. donovani* for the indicated time periods and analyzed for Egr1 ChIP assay. PCR amplification of anti-Egr1 immunoprecipitates (*IP*) and total input chromatin are shown in the *upper* and *lower panels*, respectively. *K* and *L,* macrophages were transfected (24 h) with either control or Egr1 siRNA followed by infection with *L. donovani* promastigotes for 6 h. Expression of Egr1 (*K*) and SOCS1 and SOCS3 (*L*) was evaluated by immunoblot analysis. Results are representative of three individual experiments, and the *error bars* represent mean ± S.D. ($n = 3$). *, $p < 0.05$; **, $p < 0.01$; ***, $p < 0.001$ by Student's *t* test.

ably reduced by treatment with respective siRNAs (69.2 and 81.2% reduction for SOCS1 and SOCS3, respectively, $p < 0.01$) as compared with control siRNA treatment. To see the collective role of both SOCS1 and SOCS3 on the modulation of the apoptotic cascade by *L. donovani*, we used a combined knockdown system for SOCS1 and SOCS3 for all of our experiments.

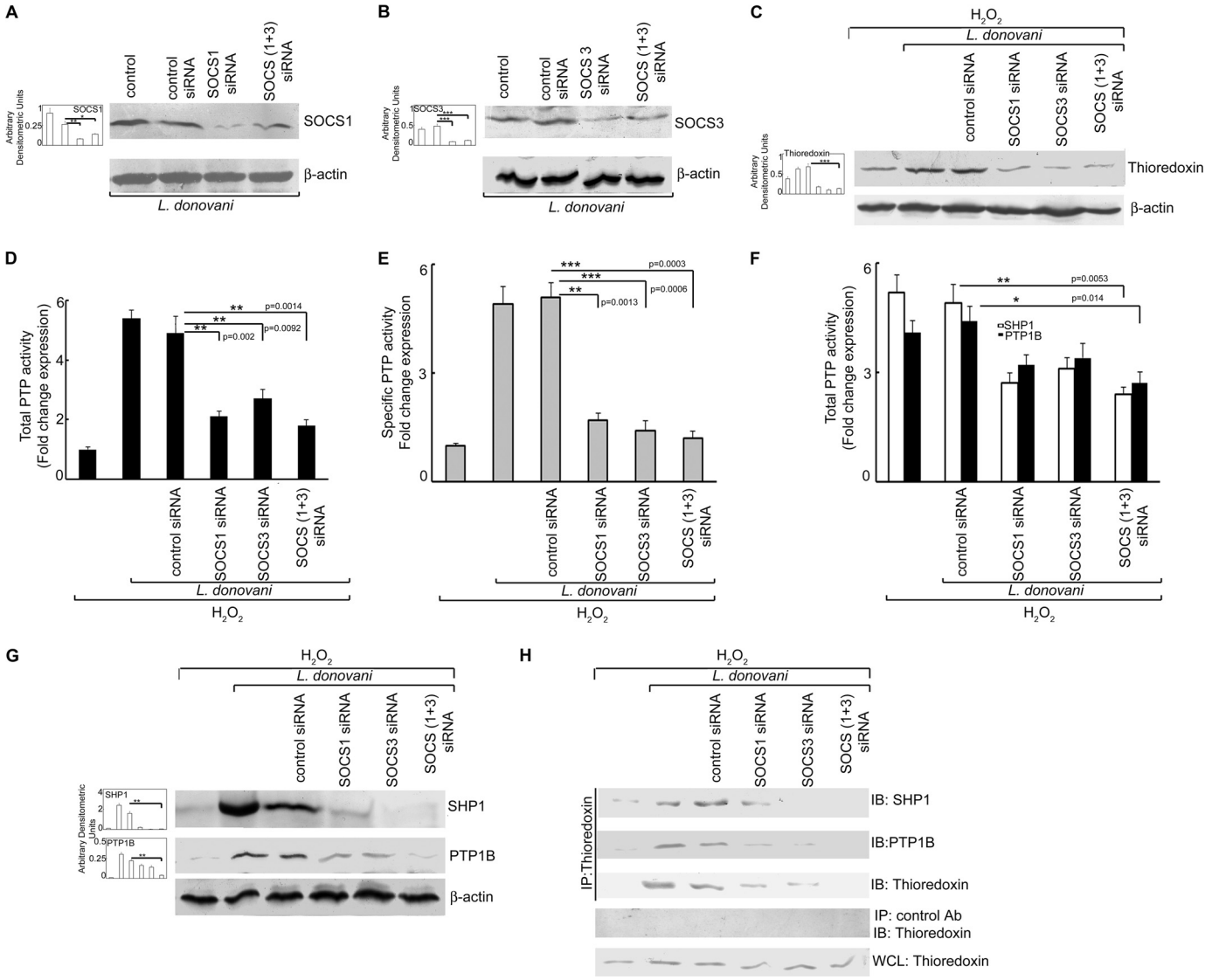

FIGURE 5. **Effect of knockdown of SOCS on macrophage PTP activity and caspase cascade.** *A* and *B*, RAW 264.7 macrophages were transfected (24 h) with either control or SOCS1 and/or SOCS3 siRNA followed by infection with *L. donovani* promastigotes for 6 h. Expression of SOCS1 (*A*) and SOCS3 (*B*) was evaluated by immunoblot analysis. *C* and *G*, expression of thioredoxin (*C*) and SHP-1 and PTP1B (*G*) was measured by Western blotting. *D* and *E*, total and specific PTP activities were evaluated by the capacity of cell lysates to hydrolyze pNPP (*D*) or a synthetic tyrosine phosphopeptide (*E*). Absorbance values were taken at 405 and 620 nm, respectively. *F*, SHP-1 and PTP-1B activities were evaluated by the capacity of immunoprecipitated phosphatases to hydrolyze pNPP. Absorbance value was taken at 405 nm. Results are expressed as the relative increase (*n*-fold) over PTP activity in control cells. *H*, cells were processed as in *A* followed by immunoprecipitation with thioredoxin antibody and immunoblotting with indicated antibodies. 30 μg of each sample was loaded as a whole cell lysate input control. *IP*, immunoprecipitation using the indicated antibody; *IB*, immunoblot analysis using the indicated antibody; *WCL*, whole cell lysate. Results are representative of three individual experiments, and the *error bars* represent mean ± S.D. ($n = 3$). *, $p < 0.05$; **, $p < 0.01$; ***, $p < 0.001$ by Student's *t* test.

Combined siRNA treatment resulted in 46.2 and 75.1% reduction in SOCS1 and SOCS3, respectively ($p < 0.05$) (Fig. 5, *A* and *B*). SOCS knockdown cells showed markedly decreased thioredoxin levels (79.4% reduction in combined SOCS1/3 siRNA-treated cells as compared with control siRNA treatment) thereby suggesting that the expression of both SOCS1 and SOCS3 is a necessary prerequisite for thioredoxin induction (Fig. 5*C*). Consistent with these data, SOCS1/3 knockdown also resulted in marked reduction in PTP activity (63.3 and 76.5% reduction in total and specific PTP activity, respectively, $p < 0.01$) (Fig. 5, *D* and *E*) as well as reduction in the activity of both SHP-1 and PTP1B (55.1 and 38.6% reduction, respectively, as compared with control siRNA treatment, $p < 0.05$) (Fig. 5*F*). We also checked the expression of both SHP-1 and PTP1B at protein level and found 93.5 and 81.9% reduction in their levels, respectively ($p < 0.01$) (Fig. 5*G*). The decrease in thioredoxin-mediated PTP activity was further validated by checking the protein-protein interaction of thioredoxin with SHP-1 and PTP1B. Co-immunoprecipitation studies revealed strong association of thioredoxin with SHP-1 and PTP1B following infection, which was markedly reduced in the presence of SOCS1/3 siRNA (Fig. 5*H*). These results indicate that both SOCS1 and SOCS3 play a vital role in thioredoxin-mediated enhancement of PTP activity in H_2O_2-treated infected macrophages.

Effect of SOCS Knockdown on MAPK-mediated Caspase Activation, Macrophage Apoptosis, and Parasite Survival—To ascertain the functional significance of SOCS in H_2O_2-treated

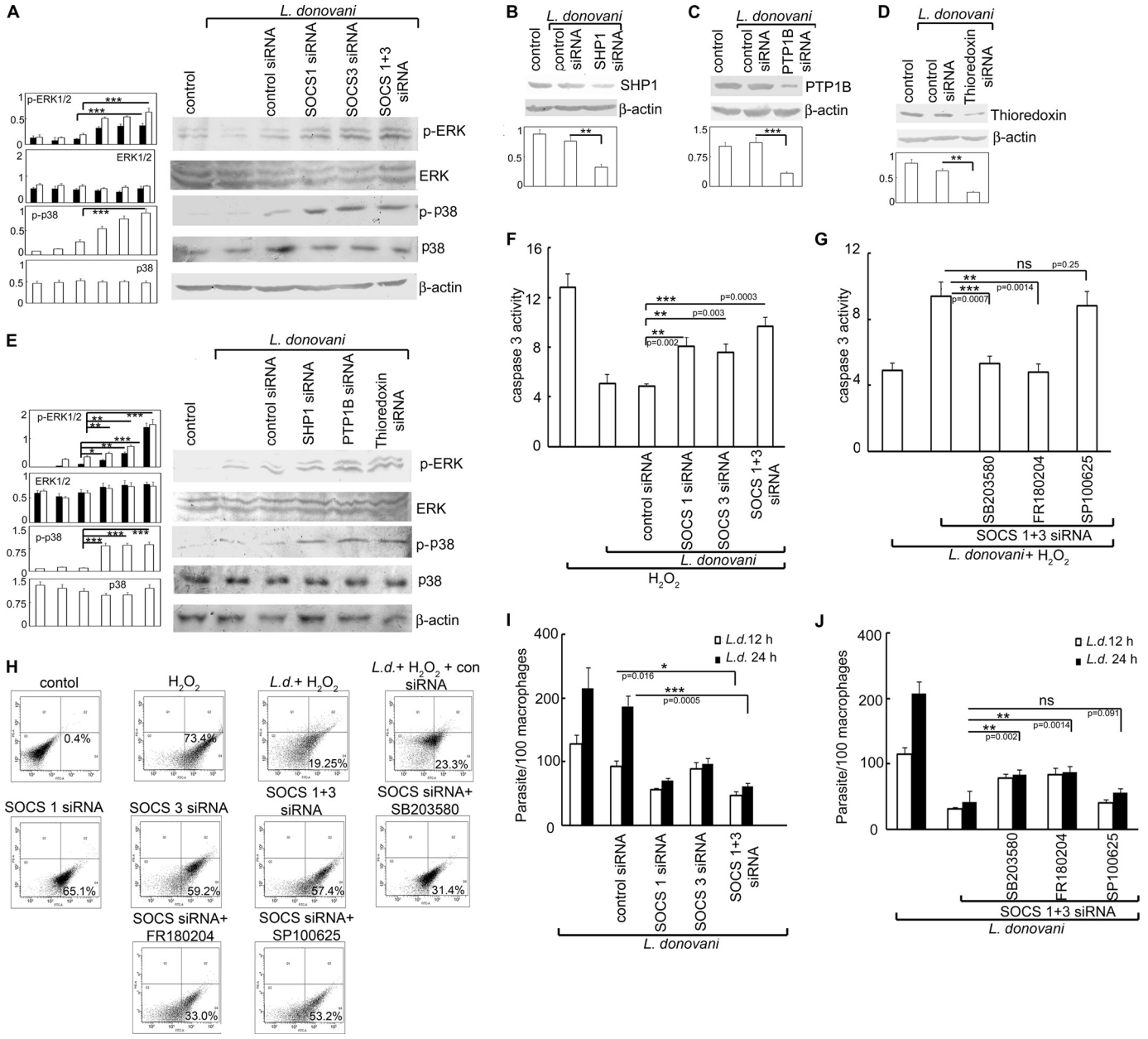

FIGURE 6. **Effect of inhibition of SOCS, thioredoxin, and PTP on MAPK activation, apoptosis, and parasite survival.** *A,* macrophages were transfected (24 h) with either control or SOCS1 and/or SOCS3 siRNA followed by infection with *L. donovani* promastigotes for 6 h. Expression of various MAPKs was evaluated by immunoblot analysis. *B–E,* macrophages were transfected (24 h) with either control or SHP1 or PTP1B or thioredoxin siRNA followed by infection with *L. donovani* promastigotes for 6 h. Expression of SHP1 (*B*), PTP1B (*C*), thioredoxin (*D*), and various MAPKs (*E*) were evaluated by immunoblotting. *F* and *G,* macrophages were transfected (24 h) with either control or SOCS1 and/or SOCS3 siRNA and preincubated with either SB203580 (10 μM) or SP100625 (10 μM) or FR180204 (10 μM) followed by infection with *L. donovani* promastigotes for 6 h. H_2O_2 was administered as described previously. Total cellular extracts (10 μg of protein per sample) were used to determine caspase-3 activity using Ac-DEVD-*p*NA as substrate. *H–J,* cells were treated as in *F* and *G,* and the percentage of apoptotic cells was measured by flow cytometry (*H*), and intracellular parasite number was determined by Giemsa staining (*I* and *J*). Results are representative of three individual experiments, and the *error bars* represent mean ± S.D. ($n = 3$). *ns*, not significant; *, $p < 0.05$; **, $p < 0.01$; ***, $p < 0.001$ by Student's *t* test.

L. donovani-infected cells, we examined the effect of SOCS knockdown on the MAPK-triggered caspase cascade and subsequent apoptotic parameters. SOCS1 and -3 silencing in *L. donovani*-infected cells led to enhanced expression of both p-p38 and p-ERK (3.1-, 3.4-, and 3.3-fold for p-p38, p-ERK1, and p-ERK2, respectively, over control siRNA-treated samples) (Fig. 6*A*). Because the de-phosphorylation of MAPKs, observed in case of *Leishmania* infection, may be mediated by thioredoxin, SHP1, and PTP1B, we studied the effect of silencing these proteins through the siRNA-mediated knockdown system on the activation of p38 and ERK in infected macrophages. Efficacy of siRNA was determined by Western blotting, which showed 59.2, 70.1, and 67.2% inhibition in the case of SHP1, PTP1B, and thioredoxin, respectively (Fig. 6, *B, C,* and *D*). Knockdown of SHP1, PTP1B, and thioredoxin led to an increase of 7.2-, 7.4-, and 7.7-fold of p-p38, 2.1-, 2.3-, and 3.4-fold of p-ERK1 and 2.3-, 2.7-, and 4.2-fold of pERK2, respectively, over control siRNA-treated samples (Fig. 6*E*) thereby suggesting that the increase in phosphatase activity in *L. donovani*-infected cells might lead to the reduction in phosphory-

lated forms of p38 and ERK1/2. SOCS1/3 silencing either alone or in combination in *L. donovani*-infected cells depicted considerable enhancement in caspase-3 activity (3.2-, 2.7-, and 4.8-fold more than control siRNA-treated cells, in the case of SOCS1, SOCS3, and SOCS1 and -3 knockdown, respectively, $p < 0.01$) (Fig. 6*F*). It was interesting to note that this increase in caspase-3 activity could be markedly reversed by administration of SB203580 and FR180204, inhibitors of p38 and ERK, respectively, thereby suggesting the active involvement of these two MAPKs in SOCS-mediated signaling (Fig. 6*G*). A comparison of apoptotic populations between control and SOCS siRNA-treated infected macrophages showed enhanced apoptosis in the latter upon H_2O_2 treatment (65.1, 59.2, and 57.4% apoptotic cells, in case of SOCS1, SOCS3, and SOCS1 and -SOCS3 knockdown, respectively, compared with 23.3% in control siRNA-treated cells) (Fig. 6*H*). In agreement with the previous data, administration of SB203580 and FR180204 resulted in marked reduction in apoptosis induced by SOCS1 and/or SOCS3 knockdown, whereas treatment with SP600125, the inhibitor of JNK, did not have any effect on the same (Fig. 6*H*). We then tried to evaluate whether this increase in apoptosis by SOCS knockdown could actually play a role in decreasing the persistence of infection. It was observed that silencing of SOCS1 and -3 either alone or simultaneously resulted in decreased intra-macrophage survival of parasites (62.1, 48.1, and 67.3% reduction in case of SOCS1, SOCS3, and SOCS1 and -3 knockdown, respectively, as compared with control siRNA treatment) (Fig. 6*I*). Moreover, administration of inhibitors for p38 and ERK along with SOCS siRNA resulted in reversal of apoptotic inhibition (Fig. 6*J*), thereby revealing an active participation of both p38 and ERK in the SOCS-mediated anti-apoptotic signaling. Collectively, all these results suggest that *L. donovani* may counteract oxidative burst-mediated apoptosis through up-regulation of SOCS1 and -3, thus allowing successful replication and survival of the parasites.

DISCUSSION

For the successful survival of intracellular pathogens, protection of their niche, *i.e.* the host cell, is a necessary prerequisite. Apoptosis of infected cells is one of the classical defense mechanisms that result in elimination of the host cell along with the pathogen (34). Hence, many pathogens, including *Leishmania,* escape immune surveillance by developing mechanisms to suppress host cell apoptosis (35). However, phagocytosis of *Leishmania* promastigotes into macrophages results in a huge oxidative burst that normally should kill the host cell resulting in parasite clearance. Although inhibition of apoptosis by *L. donovani* has been reported, the fact that the parasite is able to deal with the huge oxidative stress after being phagocytosed and can protect the host macrophages from cell death is still an unexplored area. In this study using H_2O_2 as an inducer of ROS-mediated apoptosis, we tried to elucidate the intracellular signaling mechanisms used by *L. donovani* to overcome host-cell apoptosis. We observed that *Leishmania* could prevent ROS-mediated apoptosis of macrophages through the differential induction of SOCS proteins (SOCS1 and SOCS3) through thioredoxin in the inhibition of the apoptotic cascade. Because thioredoxin has a role in PTP stabilization, it might be possible that *L. donovani* may induce thioredoxin to protect the PTPs from being oxidized by ROS, thereby inhibiting the MAPK-driven caspase cascade.

The involvement of ROS in inducing cell death has been demonstrated in a number of studies (36, 37). In this study, we demonstrated that H_2O_2, which induces apoptosis in normal cells, could not do so in *L. donovani*-infected macrophages despite increased levels of ROS. *Leishmania* may achieve apoptotic inhibition via neutralization of ROS-mediated apoptotic signaling cascade rather than decreasing ROS production itself. Caspases that perform critically important roles in the induction of apoptosis are primarily triggered via two distinct but interconnected pathways, namely the mitochondrion-mediated and death receptor pathways (38). Both of these pathways eventually merge and lead to the activation of the downstream effector caspases-3 and -7, which ultimately execute apoptosis of the cell (38). In this study, we found that *Leishmania* markedly reduced the expression of both active initiator caspases-9 and -7 followed by suppression of the effector caspase-3 in host cells. MAPKs are known to have a precise role in the initiation of the caspase cascade, and there is evidence regarding their involvement in cleaving of inactive caspases, thus rendering them active. Our study also revealed a significant reduction in the phosphorylation of ERK and p38 in *L. donovani* infection. MAPKs in turn are known to be regulated by PTPs; therefore, we studied the role of PTP in the MAPK-mediated apoptotic signaling cascade. ROS is reported to cause PTP inactivation by attacking thiol groups in the catalytic site of the PTP (39). The essential role of the active site cysteine residue in PTP-mediated catalysis provides a mechanism for redox-based regulation of PTP activity. The reversible oxidation and inactivation of PTP in response to H_2O_2 provide a well established mechanism for control of tyrosine phosphorylation-dependent signaling. H_2O_2 exposure to control macrophages resulted in inhibition of CD45, SHP-1, SHP-2, and PTP1B with a concomitant activation of ERK and p38. We found an enhancement of the specific activities of SHP-1 and PTP-1B following infection, which might contribute to de-phosphorylation of MAPK and consequent inhibition of the caspase cascade. However, the precise role that individual MAPK members play during ROS-induced apoptosis requires further investigation.

PTPs are known to be stabilized by a number of enzymes of the ROS-scavenging system. Thioredoxin might be involved in the stabilization of PTPs in *Leishmania* infection as its levels are increased in infected macrophages. The enhanced association of thioredoxin with SHP1 and PTP-1B may lead to the protection of thiol groups from ROS attack. The results of some recent studies demonstrate the role of SOCS family members in regulating thioredoxin expression during oxidative stress conditions. Moreover, SOCS1-transduced cells display elevated thioredoxin levels and a decrease in ROS generation induced by oxidative stress (27). Although specific interactions of SOCS1 with the transcription machinery of thioredoxin genes are not known, the role of SOCS proteins as transcriptional factors has been suggested in recent studies. This study indicated that infection by *L. donovani* resulted in induced expression of both SOCS1 and SOCS3 in macrophages, and transcription of these proteins may be regulated by the transcription factor Egr1.

TGF-β has been reported to induce rapid induction of Egr1 in human skin fibroblasts (40), aortic smooth muscle cells (41), and mouse embryonic fibroblasts (42). Incidentally, *L. donovani* infection leads to the production of TGF-β, which is one of the major players in generating a Th2-biased immune response for establishment of infection (43, 44). It might be possible that during infection, high levels of TGF-β may be exploited by *Leishmania* to induce Egr1 levels. Our findings suggest that both SOCS1 and SOCS3 have a role in the inhibition of host cell apoptosis by *L. donovani*, which may be mediated through the induction of thioredoxin, which protects PTPs. These findings seem to be in good agreement with the fact that SOCS induction is correlated with cyto-protection (45). A number of emerging studies have revealed the implication of SOCS proteins in the regulation of cellular proliferation and apoptosis. For example, abolition of SOCS gene expression has been reported to induce apoptosis in liver and lymphoid organs (46, 47). To understand the mechanism responsible for increased apoptosis after SOCS down-regulation, we looked for changes in the expression levels of thioredoxin and phosphorylation of MAPKs and found that SOCS knockdown was correlated with increased phosphorylation of ERK and p38. Increased apoptosis was associated with activation of pro-apoptotic caspase-3, caspase-7, and caspase-9, and increased levels of cleaved poly(ADP-ribose) polymerase. Functional knockdown of SOCS resulted in reduced expression of thioredoxin suggesting a direct correlation between SOCS proteins and thioredoxin. In this context, we also observed a decrease in endogenous PTP activation in SOCS-siRNA-treated macrophages along with enhanced apoptosis of infected macrophages. However, either SOCS1 or SOCS3 did not co-immunoprecipitate with thioredoxin, SHP1, and PTP1B (supplemental Fig. 3) suggesting that SOCS do not directly associate with these proteins. SOCS1 has been reported to be associated with thioredoxin transcription as observed by elevated thioredoxin mRNA levels in SOCS1-overexpressing cells (27). It might therefore be possible that in *L. donovani*-infected macrophages, induced expression of SOCS led to enhanced thioredoxin transcription, thereby stabilizing the PTPs. The role of SOCS proteins during infection by various intracellular pathogens has been reported in a number of studies. For example, *T. gondii* induces endogenous SOCS1 and CIS, and this contributes to the parasite's inhibition of IFN-γ (48). Also, infection with *L. monocytogenes* modulated IFN-γ signaling via induction of SOCS-3 (49). Our findings coincided with these reports as SOCS down-regulation resulted in decreased parasite survival thereby suppressing disease progression. Taken together, this study demonstrated that SOCS proteins play an important role in stabilizing the survival machinery of infected cells in the course of phagocytosis, and their down-regulation leads to increased cell death and diminished persistence of infection. This may provide a basis for a more rational design of therapies against visceral leishmaniasis.

REFERENCES

1. Carratelli, C. R., Rizzo, A., Catania, M. R., Gallè, F., Losi, E., Hasty, D. L., and Rossano, F. (2002) *Chlamydia pneumoniae* infections prevent the programmed cell death on THP-1 cell line. *FEMS Microbiol Lett.* **215,** 69–74
2. Vaux, D. L., Haecker, G., and Strasser, A. (1994) An evolutionary perspective on apoptosis. *Cell* **76,** 777–779
3. Campanella, M., de Jong, A. S., Lanke, K. W., Melchers, W. J., Willems, P. H., Pinton, P., Rizzuto, R., and van Kuppeveld, F. J. (2004) The coxsackievirus 2B protein suppresses apoptotic host cell responses by manipulating intracellular Ca^{2+} homeostasis. *J. Biol. Chem.* **279,** 18440–18450
4. Fiorentini, C., Falzano, L., Travaglione, S., and Fabbri, A. (2003) Hijacking Rho GTPases by protein toxins and apoptosis: molecular strategies of pathogenic bacteria. *Cell Death Differ.* **10,** 147–152
5. Grassmé, H., Jendrossek, V., and Gulbins, E. (2001) Molecular mechanisms of bacteria induced apoptosis. *Apoptosis* **6,** 441–445
6. Barry, M., and Bleackley, R. C. (2002) Cytotoxic T lymphocytes: all roads lead to death. *Nat. Rev. Immunol.* **2,** 401–409
7. Roulston, A., Marcellus, R. C., and Branton, P. E. (1999) Viruses and apoptosis. *Annu. Rev. Microbiol.* **53,** 577–628
8. Gao, L. Y., and Kwaik, Y. A. (2000) The modulation of host cell apoptosis by intracellular bacterial pathogens. *Trends Microbiol.* **8,** 306–313
9. Sinai, A. P., Payne, T. M., Carmen, J. C., Hardi, L., Watson, S. J., and Molestina, R. E. (2004) Mechanisms underlying the manipulation of host apoptotic pathways by *Toxoplasma gondii*. *Int. J. Parasitol.* **34,** 381–391
10. Schaumburg, F., Hippe, D., Vutova, P., and Lüder, C. G. (2006) Pro- and anti-apoptotic activities of protozoan parasites. *Parasitology* **132,** S69–S85
11. Shim, J. H., Xiao, C., Paschal, A. E., Bailey, S. T., Rao, P., Hayden, M. S., Lee, K. Y., Bussey, C., Steckel, M., Tanaka, N., Yamada, G., Akira, S., Matsumoto, K., and Ghosh, S. (2005) TAK1, but not TAB1 or TAB2, plays an essential role in multiple signaling pathways *in vivo*. *Genes Dev.* **19,** 2668–2681
12. Eley, A., Hosseinzadeh, S., Hakimi, H., Geary, I., and Pacey, A. A. (2005) Apoptosis of ejaculated human sperm is induced by co-incubation with *Chlamydia trachomatis* lipopolysaccharide. *Hum. Reprod.* **20,** 2601–2607
13. Sukumaran, S. K., Selvaraj, S. K., and Prasadarao, N. V. (2004) Inhibition of apoptosis by *Escherichia coli* K1 is accompanied by increased expression of BclXL and blockade of mitochondrial cytochrome *c* release in macrophages. *Infect. Immun.* **72,** 6012–6022
14. Park, J. S., Tamayo, M. H., Gonzalez-Juarrero, M., Orme, I. M., and Ordway, D. J. (2006) Virulent clinical isolates of *Mycobacterium tuberculosis* grow rapidly and induce cellular necrosis but minimal apoptosis in murine macrophages. *J. Leukocyte Biol.* **79,** 80–86
15. Nash, P. B., Purner, M. B., Leon, R. P., Clarke, P., Duke, R. C., and Curiel, T. J. (1998) *Toxoplasma gondii*-infected cells are resistant to multiple inducers of apoptosis. *J. Immunol.* **160,** 1824–1830
16. van de Sand, C., Horstmann, S., Schmidt, A., Sturm, A., Bolte, S., Krueger, A., Lütgehetmann, M., Pollok, J. M., Libert, C., and Heussler, V. T. (2005) The liver stage of *Plasmodium berghei* inhibits host cell apoptosis. *Mol. Microbiol.* **58,** 731–742
17. Moore, K. J., and Matlashewski, G. (1994) Intracellular infection by *Leishmania donovani* inhibits macrophage apoptosis. *J. Immunol.* **152,** 2930–2937
18. Ruhland, A., Leal, N., and Kima, P. E. (2007) *Leishmania* promastigotes activate PI3K/Akt signalling to confer host cell resistance to apoptosis. *Cell. Microbiol.* **9,** 84–96
19. Horta, M. F., Mendes, B. P., Roma, E. H., Noronha, F. S., Macêdo, J. P., Oliveira, L. S., Duarte, M. M., and Vieira, L. Q. (2012) Reactive oxygen species and nitric oxide in cutaneous leishmaniasis. *J. Parasitol. Res.* **2012,** 203818
20. Lind, L., and Ljunghall, S. (1992) Serum urate and renal function in different forms of hypercalcemia. *Exp. Clin. Endocrinol.* **99,** 87–90
21. Murray, H. W. (1981) Susceptibility of Leishmania to oxygen intermediates and killing by normal macrophages. *J. Exp. Med.* **153,** 1302–1315
22. Lodge, R., Diallo, T. O., and Descoteaux, A. (2006) *Leishmania donovani* lipophosphoglycan blocks NADPH oxidase assembly at the phagosome membrane. *Cell. Microbiol.* **8,** 1922–1931
23. Meng, T. C., Fukada, T., and Tonks, N. K. (2002) Reversible oxidation and inactivation of protein-tyrosine phosphatases *in vivo*. *Mol. Cell* **9,** 387–399
24. Hoffmann, K. M., Tonks, N. K., and Barford, D. (1997) The crystal structure of domain 1 of receptor protein-tyrosine phosphatase μ *J. Biol. Chem.* **272,** 27505–27508

25. Nordberg, J., and Arnér, E. S. (2001) Reactive oxygen species, antioxidants, and the mammalian thioredoxin system. *Free Radic. Biol. Med.* **31,** 1287–1312
26. Didier, C., Kerblat, I., Drouet, C., Favier, A., Béani, J. C., and Richard, M. J. (2001) Induction of thioredoxin by ultraviolet-A radiation prevents oxidative-mediated cell death in human skin fibroblasts. *Free Radic. Biol. Med.* **31,** 585–598
27. Oh, J., Hur, M. W., and Lee, C. E. (2009) SOCS1 protects protein-tyrosine phosphatases by thioredoxin upregulation and attenuates Jaks to suppress ROS-mediated apoptosis. *Oncogene* **28,** 3145–3156
28. Roberts, A. W., Robb, L., Rakar, S., Hartley, L., Cluse, L., Nicola, N. A., Metcalf, D., Hilton, D. J., and Alexander, W. S. (2001) Placental defects and embryonic lethality in mice lacking suppressor of cytokine signaling 3. *Proc. Natl. Acad. Sci. U.S.A.* **98,** 9324–9329
29. Qian, Y. R., Zhang, Q. R., Cheng, T., Wan, H. Y., and Zhou, M. (2011) RNA interference-mediated silencing of SOCS-1 via lentiviral vector promotes apoptosis of alveolar epithelial cells *in vitro*. *Mol. Med. Rep.* **5,** 452–456
30. Puhr, M., Santer, F. R., Neuwirt, H., Susani, M., Nemeth, J. A., Hobisch, A., Kenner, L., and Culig, Z. (2009) Down-regulation of suppressor of cytokine signaling-3 causes prostate cancer cell death through activation of the extrinsic and intrinsic apoptosis pathways. *Cancer Res.* **69,** 7375–7384
31. Madonna, S., Scarponi, C., Pallotta, S., Cavani, A., and Albanesi, C. (2012) Anti-apoptotic effects of suppressor of cytokine signaling 3 and 1 in psoriasis. *Cell Death Dis.* **3,** e334
32. Xiong, H., Du, W., Zhang, Y. J., Hong, J., Su, W. Y., Tang, J. T., Wang, Y. C., Lu, R., and Fang, J. Y. (2012) Trichostatin A, a histone deacetylase inhibitor, suppresses JAK2/STAT3 signaling via inducing the promoter-associated histone acetylation of SOCS1 and SOCS3 in human colorectal cancer cells. *Mol. Carcinog.* **51,** 174–184
33. Srivastav, S., Kar, S., Chande, A. G., Mukhopadhyaya, R., and Das, P. K. (2012) *Leishmania donovani* exploits host deubiquitinating enzyme A20, a negative regulator of TLR signaling, to subvert host immune response. *J. Immunol.* **189,** 924–934
34. Ashida, H., Mimuro, H., Ogawa, M., Kobayashi, T., Sanada, T., Kim, M., and Sasakawa, C. (2011) Cell death and infection: A double-edged sword for host and pathogen survival. *J. Cell Biol.* **195,** 931–942
35. Lisi, S., Sisto, M., Acquafredda, A., Spinelli, R., Schiavone, M., Mitolo, V., Brandonisio, O., and Panaro, M. (2005) Infection with *Leishmania infantum* inhibits actinomycin D-induced apoptosis of human monocytic cell line U-937. *J. Eukaryot. Microbiol.* **52,** 211–217
36. Maillet, A., Yadav, S., Loo, Y. L., Sachaphibulkij, K., and Pervaiz, S. (2013) A novel osmium-based compound targets the mitochondria and triggers ROS-dependent apoptosisin colon carcinoma. *Cell Death Dis.* **4,** e653
37. Wu, Y., Zhang, X., Kang, X., Li, N., Wang, R., Hu, T., Xiang, M., Wang, X., Yuan, W., Chen, A., Meng, D., and Chen, S. (2013) Oxidative stress inhibits adhesion and transendothelial migration and induces apoptosis and senescence of induced pluripotent stem cells. *Clin. Exp. Pharmacol. Physiol.* **40,** 626–634
38. Chowdhury, I., Tharakan, B., and Bhat, G. K. (2006) Current concepts in apoptosis: the physiological suicide program revisited. *Cell. Mol. Biol. Lett.* **11,** 506–525
39. Denu, J. M., and Tanner, K. G. (1998) Specific and reversible inactivation of protein-tyrosine phosphatases by hydrogen peroxide: evidence for a sulfenic acid intermediate and implications for redox regulation. *Biochemistry* **37,** 5633–5642
40. Chen, S. J., Ning, H., Ishida, W., Sodin-Semrl, S., Takagawa, S., Mori, Y., and Varga, J. (2006) The early-immediate gene EGR-1 is induced by transforming growth factor-β and mediates stimulation of collagen gene expression. *J. Biol. Chem.* **281,** 21183–21197
41. Fu, M., Zhang, J., Lin, Y., Zhu, X., Zhao, L., Ahmad, M., Ehrengruber, M. U., and Chen, Y. E. (2003) Early stimulation and late inhibition of peroxisome proliferator-activated receptor γ (PPARγ) gene expression by transforming growth factor β in human aortic smooth muscle cells: role of early growth-response factor-1 (Egr-1), activator protein 1 (AP1) and Smads. *Biochem. J.* **370,** 1019–1025
42. Bhattacharyya, S., Ishida, W., Wu, M., Wilkes, M., Mori, Y., Hinchcliff, M., Leof, E., and Varga, J. (2009) A non-Smad mechanism of fibroblast activation by transforming growth factor-β via c-Abl and Egr-1: selective modulation by imatinib mesylate. *Oncogene* **28,** 1285–1297
43. Somanna, A., Mundodi, V., and Gedamu, L. (2002) Functional analysis of cathepsin B-like cysteine proteases from *Leishmania donovani* complex. Evidence for the activation of latent transforming growth factor β. *J. Biol. Chem.* **277,** 25305–25312
44. Wilson, M. E., Young, B. M., Davidson, B. L., Mente, K. A., and McGowan, S. E. (1998) The importance of transforming growth factor-β in murine visceral leishmaniasis. *J. Immunol.* **161,** 6148–6155
45. Duval, D., Reinhardt, B., Kedinger, C., and Boeuf, H. (2000) Role of suppressors of cytokine signaling (Socs) in leukemia inhibitory factor (LIF) -dependent embryonic stem cell survival. *FASEB J.* **14,** 1577–1584
46. Naka, T., Matsumoto, T., Narazaki, M., Fujimoto, M., Morita, Y., Ohsawa, Y., Saito, H., Nagasawa, T., Uchiyama, Y., and Kishimoto, T. (1998) Accelerated apoptosis of lymphocytes by augmented induction of Bax in SSI-1 (STAT-induced STAT inhibitor-1) deficient mice. *Proc. Natl. Acad. Sci. U.S.A.* **95,** 15577–15582
47. Starr, R., Metcalf, D., Elefanty, A. G., Brysha, M., Willson, T. A., Nicola, N. A., Hilton, D. J., and Alexander, W. S. (1998) Liver degeneration and lymphoid deficiencies in mice lacking suppressor of cytokine signaling-1. *Proc. Natl. Acad. Sci. U.S.A.* **95,** 14395–14399
48. Zimmermann, S., Murray, P. J., Heeg, K., and Dalpke, A. H. (2006) Induction of suppressor of cytokine signaling-1 by *Toxoplasma gondii* contributes to immune evasion in macrophages by blocking IFN-γ signaling. *J. Immunol.* **176,** 1840–1847
49. Yamamoto, K., Kawamura, I., Tominaga, T., Nomura, T., Kohda, C., Ito, J., and Mitsuyama, M. (2005) Listeriolysin O, a cytolysin derived from *Listeria monocytogenes*, inhibits generation of ovalbumin-specific Th2 immune response by skewing maturation of antigen-specific T cells into Th1 cells. *Clin. Exp. Immunol.* **142,** 268–274